UC San Diego

Title

How the birth and death of shear layers determine confinement evolution: from the L H transition to the density limit

Permalink

https://escholarship.org/uc/item/6rn7j1f9

Journal

Philosophical Transactions of the Royal Society A Mathematical Physical and Engineering Sciences, 381(2242)

ISSN

1364-503X

Authors

Diamond, Patrick H
Singh, Rameswar
Long, Ting
et al.

Publication Date

2023-02-20

DOI

10.1098/rsta.2021.0227

PHILOSOPHICAL TRANSACTIONS A

Research

CrossMark
click for updates

Author for correspondence:

P.H. Diamond

e-mail: pdiamond@ucsd.edu

How the Birth and Death of Shear Layers Determine Confinement Evolution: From the L → H Transition to the Density Limit

[1]P.H. Diamond, [1]Rameswar Singh, [2]Ting Long, [3]Rongjie Hong, [2]Rui Ke, [4]Zheng Yan, [1]Mingyun Cao, [1]G.R. Tynan

[1]University of California, San Diego; San Diego, USA
[2]Southwestern Institute of Physics; Chengdu, China
[3]University of California, Los Angeles; Los Angeles, California
[4]University of Wisconsin, Madison; Wisconsin, USA

Electric field profile structure—especially its shear—is a natural order parameter for the edge plasma, and characterizes confinement regimes ranging from the H-mode [1] to the density limit [2]. The theoretical developments and lessons learned during 40 years of H-mode studies [3,4] are applied to the shear layer collapse paradigm [5] for the onset of density limit phenomena. Results from recent experiments on edge shear layers and density limit phenomenology are summarized and discussed in the light of L → H transition physics. The theory of shear layer collapse is then developed. We demonstrate that shear layer physics captures both the well known current (Greenwald) scaling of the density limit [6,7], as well as the emerging power scaling [8]. The derivation of the power scaling theory exploits an existing model, originally developed for the L → H transition [9,10]. We describe the enhanced particle transport events which occur following shear layer collapse. Open problems and future directions are discussed.

1. Introduction

2022 marks the passage of 40 years of L → H transition studies. The H-mode has revolutionized magnetic confinement physics and plasma physics, in general.

THE ROYAL SOCIETY
PUBLISHING

2

rsta.royalsocietypublishing.org Phil. Trans. R. Soc. A 0000000

Accessing the H-mode rescued toroidal confinement from its wanderings in the wildness of pessimistic scalings proposed by Goldston [11] and others, and guided it to a new world of reduced transport losses. Studies of the L → H transition introduced the concepts of transport barriers [12] and transport bifurcations [13] to confinement physics. These initiated a new way of thinking about transport—as states of transport and profiles, interleaved by spatiotemporally evolving transitions [10,14]. The H-mode taught us to appreciate the crucial role of *flow profile structure* in confinement [15]. $E \times B$ flow *shear* [16] is the most frequently studied aspect of flow profile structure, but flow curvature [17] is also of some interest. Consideration of confinement phase transitions naturally led to the identification of dynamical feedback loops, such as those in predator-prey models [9]. These are now used routinely in transition and confinement modelling, and have been applied to zonal flows in magnetized plasmas [18,19], geophysical fluids [20], and to pipe flow [21]. The L → H transition has led us to novel, 'limit cycle' states [22,23], and to consideration of back transitions and hysteresis [23]. Of course, the H-mode also forced us to confront the consequences of marked transport reduction, most notably Edge Localized Modes (ELMs) [24]. The desire to mitigate or suppress ELMs spawned a host of H-mode variants, such as Quiescent H-mode (QH-mode) [25], Improved-mode (I-mode) [26], Wide Pedestal Quiescent H-mode (WPQH-mode) [27], Resonant Magnetic Perturbation H-mode (RMPH-mode) [28], etc. just to name a few. More generally, we now pursue states of good confinement with good power handling, and boundary control [29], instead of seeking to optimize confinement alone. The goal now is transport regulation, not transport elimination.

Many of the lessons learned in the study of the L → H transition have applications to other topics in confinement physics. Indeed, such broad applicability is an indicator of the importance of these ideas. This paper deals with one such area of 'broader impact', namely that of the transport physics of the density limit. Density limits are crucial to burning plasmas, since high density burning regimes are naturally desirable, and because the density limit constrains the possible operating space. Of course, density limits are a well-established topic, and traditionally are associated with radiative cooling [2,6], and its interaction with tearing modes and disruption [30]. However, recent experiments have reinforced early suggestions that particle transport, especially at the edge, plays an important role in limiting density [31]. A reduction or collapse of the universally present edge shear layer has been linked to the occurrence of enhanced particle transport events approaching the density limit [32]. Theory relates increased collisionality and edge cooling to decreased adiabaticity ($\alpha = k_{\parallel}^2 v_{the}^2 / \omega \nu_{e,e}$, where $k_{\parallel}$ is the wave vector of the drift wave in the direction parallel to the magnetic field, v_{the} is the electron thermal velocity, ω is the frequency of the drift wave, and $\nu_{e,e}$ is the electron-electron collision rate.) and thus to a concomitant reduction in zonal flow production [33,34]. And density limits are richer than the long standing and well known Greenwald scaling $\bar{n}_G \sim I_p/a^2$, where I_p is the plasma current, and a is the minor radius. Non-trivial power scaling is now observed [8]. All told, the body of density limit transport phenomenology naturally leads itself to description as a confinement phase transition, with flow-turbulence feedback, etc. Thus it is a natural place to apply the lessons learned from the study of the L → H transition. For this reason, it is the focus of this paper, written for the occasion of 40 years of H-mode.

In this "perspective" paper, we discuss the transport physics of the density limit, with special focus on the application of ideas from confinement phase transition models. We summarize the recent phenomenology to formulate the 'shear layer collapse scenario', and discuss its link to adiabaticity α. Recent interesting electrode bias experiments are discussed. The relation of shear flow evolution to enhanced particle transport events at the density limit is demonstrated. Theoretical work focuses on linking microphysics to macroscopic scalings. Greenwald scaling is shown to follow from neoclassical dielectric screening effects on the zonal flow response [35]. A predator-prey model is developed to predict zonal flow collapse. We identify a dimensionless parameter which characterizes the collapse onset. By exploiting and extending the Kim-Diamond model of the L → H transition, we derive the scaling relation $n_{crit} \sim Q_i^{1/3}$ for ITG turbulence [36]. Here n_{crit} is the critical edge density for zonal flow collapse and Q_i is the edge ion heat flux. This

is consistent with empirical power scalings of the density limit, and may suggest the existence of a higher density limit in burning plasmas, which are strongly self-heated. A novel form of hysteresis in n_{crit} vs Q_i is predicted. Throughout this 'perspective' paper, we emphasize connections between the transport physics of the density limit and the physics of the L → H transition.

The remainder of this paper is organized as follows. Section 2 presents the physics of density limits, from a transport perspective. In section 3, we discuss results from recent experiments, with special focus on the relation between particle transport events and shear layer collapse. Section 4 explains the theory of density limit scaling. The foci are plasma current (Greenwald) and power scalings. In section 5, we discuss the H-mode density limit. Section 6 gives a comprehensive summary and discussion. Section 7 is the conclusion.

2. Physics of Density Limits—a Transport Perspective

Fusion gain increases as the square of density. Thus, burning plasma devices are planned to operate in high density regimes. It's no surprise, then, that the long-standing question of the density limit is re-emerging as a key issue in magnetic confinement. Several recent experiments and related theories have suggested that the conventional wisdom of the density limit may be seriously incomplete, or even incorrect. Here, the conventional wisdom is the well known empirical Greenwald scaling for the line averaged density $\bar{n}$, i.e. $\bar{n} = \bar{n}_G \sim I_p/a^2$, which defines a boundary for the onset of a progression of phenomena frequently terminating in disruption. Specifically, the sequence of evolution starts with edge cooling, leading to a MARFE [37], which then drives current profile contraction, which then triggers magnetic island growth and disruption. See figure 1. The details of the disruption scenarios vary [30], but all models of this
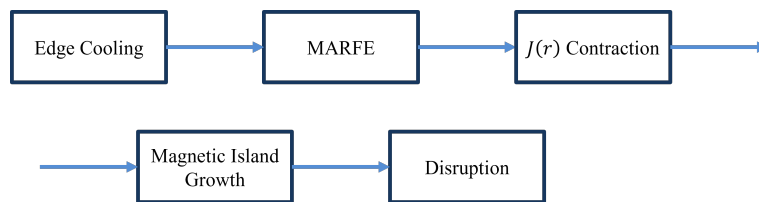

Figure 1. A schematic of a sequence of processes leading to disruption at high density.

genre involve radiative cooling and some sort of MHD. However, more than macroscopics is in play. Even the early studies of density limits observed that *edge particle transport* appeared to be important, and indeed essential—with disruption emerging as an outcome *secondary* to edge cooling by increased particle transport. From this perspective, the Greenwald limit was seen as a fundamental limit imposed by *transport*. One early experiment which pointed this way was by Greenwald on Alcator C (see figure 2) [7]. This study indicated that $\bar{n}_e$ decayed without disruption following shallow pellet injection which caused transient increases of $\bar{n}_e$ above $\bar{n}_G$. Note that the asymptotic value of $\bar{n}_e$ scales with I_p, consistent with Greenwald scaling. This result thus suggests that the density limit was enforced by *transport-induced relaxation*.

Given the apparent critical role of edge cooling and the likely importance of edge particle transport, it is useful to review a key element of the tokamak edge—namely the *edge shear layer* [38]. This is found in Ohmic and L-mode plasmas, and grows larger and stronger in H-mode. Indeed, the edge shear layer is present in all tokamaks, and has also been detected in stellarators [39]. It can be viewed as an unavoidable consequence of the transition from $E_r < 0$ inside the last closed flux surface (LCFS) to $E_r > 0$ in the SOL. The edge shear layer sits at, or adjacent to, the last closed flux surface. Even in L-mode, the edge shear layer is strong enough to locally reduce turbulence and transport. Ritz, et al. [38] discovered a drop in fluctuation
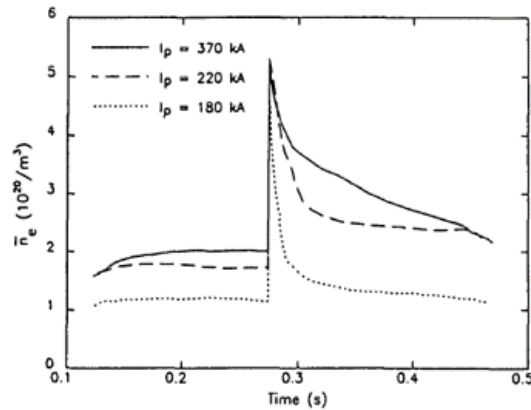
Figure 2. Electron density decays without disruption after shallow pellet injection on Alcator C. Clearly, $\bar{n}_e$ asymptote scales with I_p, which indicates that the density limit was enforced by transport induced relaxation.

correlation within the edge shear layer. The edge shear layer plays an important role in the formation of the transport barrier at the L $\rightarrow$ H transition.

Later, the edge shear layer manifested a connection to density limit physics. Several experiments [5,32,40] observed that the edge shear weakened and collapsed as $\bar{n}_e \rightarrow \bar{n}_G$. Specifically, the fluctuation Reynolds power—a measure of power coupling from fluctuations to flows—was observed to decay as $\bar{n}_e \rightarrow \bar{n}_G$, indicating a weakening of flow shear drive. Here, $P_{Re} = \langle \tilde{v}_r \tilde{v}_\theta \rangle \langle v_E \rangle'$. At the same time, turbulent fluctuations and transport increased, leading to a drop in particle confinement and the onset of edge cooling. Figure 3 and figure 4 show elements of these results. This change in confinement associated with the weakening of the shear layer
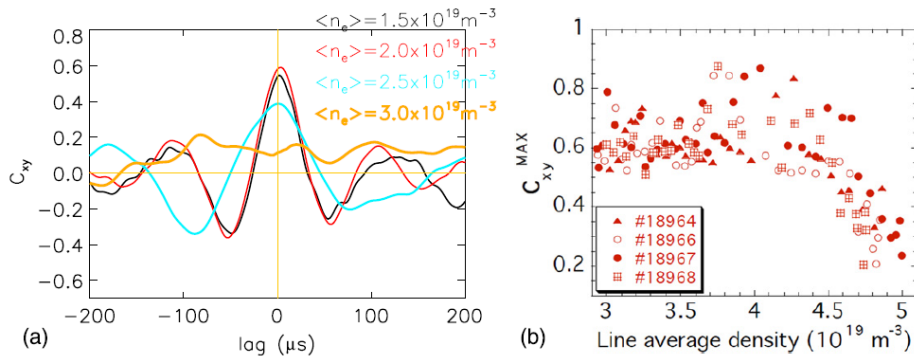

Figure 3. Decrease in maximum correlation value of LRC (long-range correlation, which denotes the zonal flow strength) as line averaged density $\bar{n}$ increases at the edge ($r/a = 0.95$) in both TEXTOR and TJ-II. The reduction in LRC due to increasing density is also accompanied by a reduction in edge mean radial electric field [32].

is somewhat reminiscent of the H $\rightarrow$ L back transition. The onset of shear layer collapse was observed to correlate with a drop in adiabaticity $\alpha = k_\parallel^2 v_{the}^2 / \omega \nu_{e,e}$ from $\alpha \gg 1$ (i.e. adiabatic electrons) to $\alpha \ll 1$ (hydrodynamic electrons). Here $\alpha \sim 1/\nu_{e,e}$ (collisionality) $\sim 1/\bar{n}_e$ [5,41]. This trend persists in recent experiments [5] (see figure 5) and database studies [42]. Figure 6 gives a schematic of the sequence of processes from density increase to edge cooling. One interpretation of the correlation of α with density limits was a proposed change in edge turbulence 'mode',
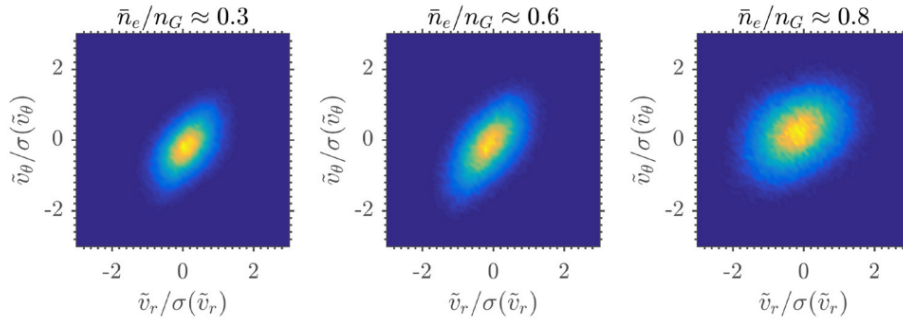
Figure 4. Joint probability distribution functions of $\tilde{V}_r$, $\tilde{V}_\theta$ for three different densities near Greenwald density limit at $r - r_{sep} = -1$ cm. Note that as $\bar{n}_e \to \bar{n}_G$, the tilt of the pdf gradually lost and the symmetry of the turbulence restored. This indicates that shear flow production by Reynolds stress was weakened. This result is consistent with the drop in Reynolds power P_{Re} observed [5].
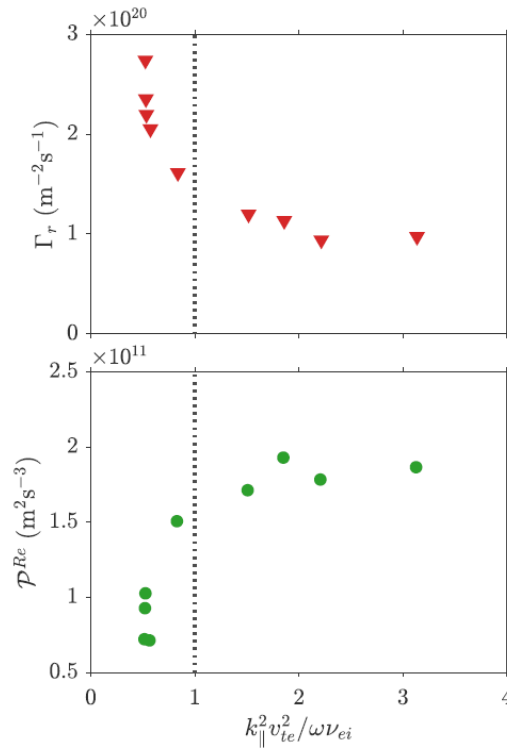

Figure 5. The plots of volume averaged particle flux (upper) and Reynolds power (bottom) as function of adiabaticity α. As α drops, the particle flux Γ_r increases while Reynolds power P_{Re} decreases. Both of these trends suggest the weakening of the shear layer [5].

from collisional drift wave ($\alpha \gg 1$) to resistive ballooning ($\alpha \ll 1$), as density and collisionality increase [33]. Here, as α increases, the basic character of the density response changes. For $\alpha \gg 1$, the density response is primarily adiabatic—i.e. electrons respond by parallel motion—so $\tilde{n}/n \sim |e| \tilde{\phi}/T_e(1 + \delta)$, as in drift waves. For $\alpha \ll 1$, the density response is primarily hydrodynamic—i.e. $\tilde{n}/n \sim (\tilde{v}_r/i\omega)(1/n)(\partial\langle n\rangle/\partial r)$—as in fluid turbulence or MHD. The change of the relative
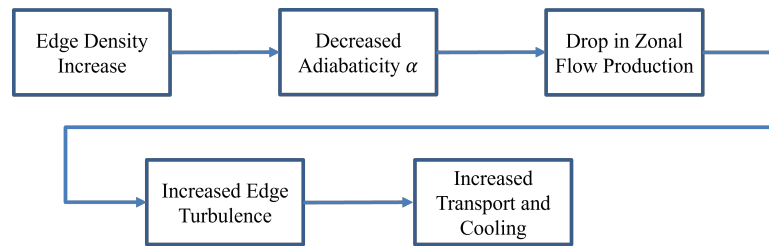
Figure 6. Schematic of processes leading to edge cooling.

phase of $\tilde{n}$ and $\tilde{v}_r$ as α transitions from large to small favors increased tranport for small α. Note that cooling raises collisionality. However, it must be stated that no distinct signature of the resistive ballooning mode (RBM) was ever observed, and that parameter studies for one experiment indicated that excitation of the RBM was unlikely [5]. An alternative, more general interpretation was advanced by Hajjar, et al. [34], who noted that shear flow production will drop as α transitions from $\alpha \gg 1$ to $\alpha \ll 1$. This is a fundamental evolutionary mechanism, applicable to a wide variety of 'modes', and thus constitutes a more robust explanation of the observations. The physics is rooted in the relation between wave energy density flux and Reynolds stress. For $\alpha \gg 1$, these two effects are closely linked. In particular, the radial wave energy density flux $S_r = v_{g_r}\mathcal{E}$ (here $\mathcal{E}$ is the wave energy density and v_{g_r} is the wave group velocity) and the Reynolds stress $\langle \tilde{v}_r \tilde{v}_\theta \rangle$ have opposite sign. Thus, we find a generic property of drift modes namely that radially outgoing waves generate flow convergences, leading to a shear flow spin-up (see figure 7). In particular, the Reynolds stress drives an influx of wave momentum which is opposite the
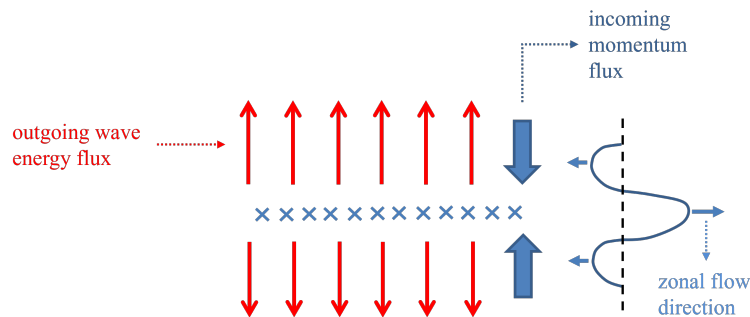

Figure 7. Here is why zonal flows are ubiquitous in drift-Rossby wave turbulence. While the group velocity, or in other words, energy density flux, of the Rossby wave is outward, its momentum flux is inward, driving the spin-up of a zonal shear layer [34].

outgoing wave energy density flux. This link is also related to the underpinning of the well known "eddy tilting" mechanism of flow generation. The flux-flow link is broken for $\alpha \ll 1$, so $\tilde{v}_r \tilde{v}_\theta$ is not simply proportional to $-S_r$, indicating that significant eddy tilting (i.e. $|\langle k_r k_\theta \rangle| \neq 0$, where $\langle \rangle$ refers to a spectral average), does not arise as a direct consequence of causality. Thus zonal flow generation weakens drastically in the $\alpha \ll 1$ regime. This is also consistent with simulation results [43,44]. These simulations all indicated a change from a state of weak drift wave turbulence and zonal flows to a state of strong vortices and hydrodynamic turbulence as α evolved from $\alpha \gg 1$ to $\alpha \ll 1$. The results are consistent with the shear flow collapse picture.

All told, these relatively recent developments have triggered the emergence of a new paradigm for the density limit—namely one linked to turbulence self-regulation and its breakdown. Of

6

rsta.royalsocietypublishing.org Phil. Trans. R. Soc. A 0000000

course, such an outlook is rooted in shear flow physics, which is fundamental to the L → H transition. This expands and generalizes the older idea of changes in linear mode. In this picture, three fundamental states of the edge plasma are possible, namely:

(i) L-mode—in which turbulence and shear flows co-exist. The shears are primarily zonal.
(ii) H-mode—with strong shear (driven by significantly ∇p) and significantly reduced turbulence. Here, the dominant contribution to the shear is from the shear of the mean electric field $\langle E_r \rangle'$.
(iii) High Density/Density Limit—in which shear flows decay, leading to higher level of turbulence and particle transport.

The edge flow shear strength emerges as a natural 'order parameter', which evolves from state-to-state, but allows a unified picture (see figure 8). In this paradigm, the transition from L → DL is seen as a kind of "back transition", i.e., a transition from L-mode to a state of even-more-degraded confinement. It should be noted, however, that the L → DL transition is not necessarily abrupt, as is expected for the first order H → L back transition. Rather, the L → DL transition is second order. Figure 8 summarizes the evolution of how we look at the density limit.
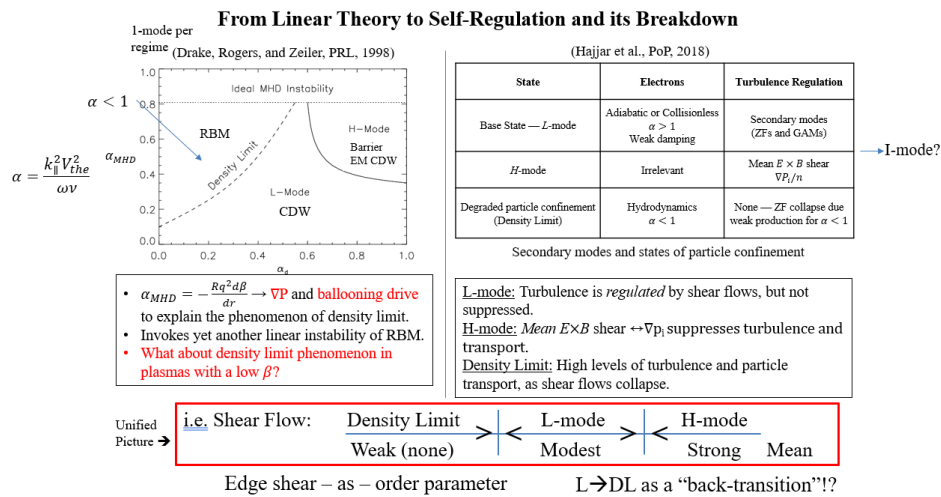

Figure 8. Evolution of the perspective on the density limit. The lower bar in red summarizes the role of shear flow [5].

3. Results from Recent Experiments

Recent experiments have aimed to test and elucidate the shear layer collapse paradigm of the density limit. As $\bar{n}_e \to \bar{n}_G$, an experiment on J-TEXT [41] observed shear layer collapse, a decrease in edge Reynolds power density, then a surge in edge particle flux and the restoration of symmetry in the velocity fluctuation probability distribution function. In particular, the ratio of Reynolds power density P_k to turbulence production by ∇n, i.e. $P_I = -c_s^2 \langle \tilde{v}_r \delta n \rangle \left((1/n_0) \, \partial \langle n \rangle / \partial r \right)$, drops as $\bar{n}_e \to \bar{n}_G$. One must ask about the fate of energy! Results indicate that the divergence of the spreading flux P_s—equivalent to a power density for turbulence spreading—increases sharply as the shear layer collapses. Here $P_s = -\partial_r \left[c_s^2 \langle \tilde{v}_r \tilde{n}^2 \rangle \right] / 2n_0^2$. Indeed, we observed that $(P_k/P_I)_{max} * (P_s/P_I)_{max} \sim constant$, suggesting that during the L → DL evolution, energy is diverted from the shear layer to the spreading flux (see figure 9). The turbulence spreading
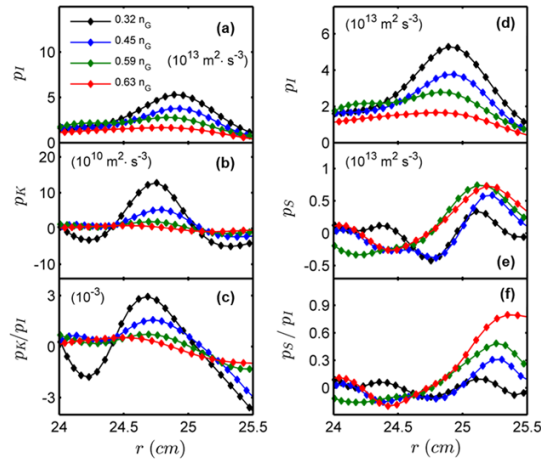
Figure 9. In standard collisionless drift wave (CDW) model, the turbulence production power from ∇n is $P_I = -c_s^2 \langle \tilde{v}_r \delta n \rangle \left((1/n_0) \, \partial \langle n \rangle / \partial r \right)$, and the Reynolds power, the power coupling to zonal flow, is $P_{Re} = P_k = \langle \tilde{v}_r \tilde{v}_\theta \rangle \langle v_E \rangle'$. Obviously, both P_I and P_k/P_I drop as $\bar{n}_e/\bar{n}_G$ rises. Meanwhile, the turbulence spreading ratio P_s/P_I enhances as $\bar{n}_e/n_G$ rises [41].

exhibits several distinct characteristics, which include:

(i) an increase in low frequency content of $\tilde{I}_{sat}/I$. Here I_{sat} is the Langmuir probe ion saturation current,

(ii) an increase in $\tilde{I}_{sat}$ autocorrelation time,

(iii) an enhanced radial correlation of $\tilde{I}_{sat}$,

(iv) the development of a positive skewness of the pdf($\tilde{I}_{sat}$),

as $\bar{n}_e \rightarrow \bar{n}_G$. Taken together, these results indicate the occurrence of enhanced turbulent particle transport events (PTE's) during L $\rightarrow$ DL evolution. PTE's are episodic, quasi-coherent density fluctuations, which result in particle transport. Thus, the usual diffusive model of turbulence spreading is not applicable here. Simulation results [45] imply that the flux $\langle \tilde{v}_r \tilde{n}\tilde{n} \rangle$ is a good indicator of the appearance of PTE's. More generally, the data suggests that the PTE's may be localized over-turning events, small avalanches [46], or "blobs" [47]. As $\bar{n}_e \rightarrow \bar{n}_G$, an increase in blob ejection has been documented previously. PTE's have been observed in particle transport experiments [48]. As is the case for prior experiments, adiabaticity $\alpha = k_\parallel^2 v_{the}^2 / \omega \nu_{e,e}$ emerged as a key parameter as in figure 5. All told, these results support the shear layer collapse scenario of L $\rightarrow$ DL, and elucidate the physics of enhanced particle transport.

At this point, it is worthwhile to compare the evolution of the shear layer collapse at the density limit to that of the L $\rightarrow$ H transition. In the shear layer collapse scenario, the drop in shear flow production triggers enhanced turbulence spreading and an increase in blob activity, as discussed above. Turbulence intensity increases at the edge, and will propagate inward. In this regard, note that if outward blob propagation increases, so must inward void propagation [46]. Thus, the turbulent region will spread inward, until the turbulence dissipates or it leads to edge cooling sufficient to trigger MHD activity. While the increase in the blob propagation at the density limit has been studied, the inward expansion of the turbulent region has not yet been examined in detail. In the L $\rightarrow$ H transition, the shear layer begins to form at the separatrix, and expands inward [22]. The evolution resembles that of a propagating turbulence quenching front, i.e. an 'anti-wake'. The front continues to propagate (so the turbulence quenching layer continues to expand) until it is blocked by the occurrence of an ELM. Thus, the motif of a 'turbulence transition

front limited by MHD' is common to both the density limit collapse and the L → H transition. It should be mentioned, though, that what ultimately limit pedestal expansion in the absence of ELMs is not yet fully understood. Neither is the evolution of the H → L back transition in the absence of ELMs [49].

The obvious question, then, is can *driving* the shear layer sustain higher densities? Is it possible to exceed the Greenwald limit using shear flow drive? [N.B.: Take care, here, to note that the H-mode density limit (HDL) is a distinct phenomenon, which involves power dependence and a strong, 'mean field' shear layer, characteristic of H-mode]. Thus, bias electrode-driven shear flows are suggested, and were investigated by Rui Ke, et al. [50]. Recall that the saga of the L → H transition includes a long history of interesting bias-driven shear flows, ranging from the early work of R.J. Taylor [51], and G.R. Tynan [52] to more recent studies by Shesterikov, et al. [53]. Electrode biasing works by generating a radial current J_r, which, in turn, drives mean poloidal rotation $\langle v_\theta \rangle$ and thus mean $E \times B$ shear $\langle v_E \rangle'$. Bias is thus an experimental 'knob' with which to vary the strength of the shear layer.

Given the background, we discuss results of recent biasing experiments on J-TEXT. As to the obligatory "What is new here?", first—the experiments are at high density, i.e. $\bar{n} \to \bar{n}_G$. Second, gas puffing is used to approach $\bar{n}_G$. Third, the experiment and analyses build on previous density limit experiments. Indeed, this experiment differs substantially from previous bias experiments, which were concerned primarily with the "bias H-mode". Results include (see figure 10):

— an observed doubling of the edge density for +240 V bias;
— $\bar{n}_{max}$ with bias > $\bar{n}_{max}$ floating, albeit modestly. Specifically, $\bar{n}_{max}$ with bias $\sim 0.7\bar{n}_G$. Thus, bias increased the operational density limit;
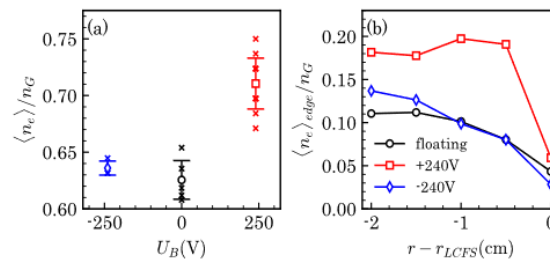— $\alpha \sim T^2/n$ systematically *increases* with bias.

Figure 10. Maximum edge density doubled for $+240$ V bias [50].

Moreover, a stronger edge shear layer resulted from positive bias. The turbulent Reynolds stress and force increased for positive bias, while $\tilde{I}_{sat}/I \sim \tilde{n}/n$ fluctuations were sharply reduced by positive bias. And not surprisingly, turbulence spreading is quenched by positive bias. All these results are quite consistent with the shear layer collapse phenomenology, and indicate that edge electrode bias regulates PTE's at high density.

In addition to the above, this experiment yielded unique insights to the "key parameter" issue for the density limit. A hysteresis study of adiabaticity α vs shearing frequency $\omega_s = \langle v_E \rangle'$ was performed, during which the bias was ramped up and down. Results are shown in figure 11. *The point is that the sense of rotation is counter-clockwise, suggesting that ω_s (shear) 'leads' α.* This suggests a causal progression: increasing shear via bias triggers a drop in turbulence and PTE activity. This in turn leads to a drop in transport and thus an *increase* in α. A tacit assumption here is that the region of interest is located in close proximity to those of the shear layer and the particle source. This result calls into question the conventional wisdom (CW) that α is 'the key parameter'. Rather, it suggests that externally driven edge shear can actually regulate α, and can be the control
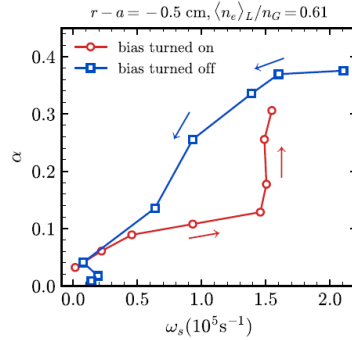
Figure 11. α vs ω_{shear} exhibits hysteresis loop during electrode bias switch on or off. N.B. the counter-clockwise direction of the trajectory in $\alpha - \omega_{shear}$ space indicates that ω_{shear} 'leads' α [50].

parameter. The CW is thus seen as representative of correlation, but not necessarily causality, especially when the shear layer is supported by external drive. Given the data supporting the α-density limit correlation [42], the α vs ω_{shear} causality issue looms large for our understanding of density limits, including the H-mode density limit. Slow bias ramps (up and down) and current ramp-down experiments are planned for the future, so as to more carefully study the physics discussed in this section.

4. Density Limit Scaling Theory

The Greenwald scaling $\bar{n}_G \sim I_p/a^2$ pervades nearly all discussions of density limits. Yet, Greenwald scaling is purely empirical, has no readily apparent physics basis, and does not emerge from an argument based upon a dimensionless ratio! While theoretical ideas—such as changes in edge turbulence mode and the connection of adiabaticity α to zonal shear collapse—capture and illuminate much of the density limit phenomenology, they do not satisfactorily address the important, "bottom line" question of the origin of Greenwald scaling (i.e. current scaling). Neither do they address the problem of *power scaling* and the physics of the L-mode density limit. Simple arguments related to radiation (and also to edge shear flow physics!) suggest that the limiting edge density n_{crit} should scale with power (or, equivalently, heat flux), i.e. $n_{crit} \sim P^\delta$, where δ is the scaling exponent. Indeed, such a trend has long been the subject of speculation, but the actual observed power dependence has usually very weak or negligible. However, recently Zanca et al. [8] showed that fits to JET data collapse to a $n_{crit} \sim P^{4/9}$ scaling (see figure 12). Later simulations claimed to agree with this trend [54,55]. Neither work presented a detailed physics picture supporting or explaining the scaling. This is an important topic, since fusion gain increases $\sim n^2$, suggesting that a feedback loop of an increased density $\rightarrow$ increased fusion power $\rightarrow$ further increased density, etc. might operate in a burning plasma. Below, we discuss recent progress and present-day issues in understanding the physics of density limit scaling. Along the way, we will discuss connections to the closely related problem of stellarator density limits.

The central issue one must confront to address the Greenwald scaling is "why current and not $q(r)$?". Greenwald scaling clearly is *not* equivalent to q scaling, which is ubiquitous in edge turbulence [56]. Consideration of this question in the light of the shear layer collapse scenario leads us to the hypothesis that the key physics lies in the neoclassical dielectric and its role in screening the zonal (shear) response [57,58]. Recall that the neoclassical dielectric scales as [59]

$$\epsilon_{neo} = 1 + \frac{4\pi\rho c^2}{B_\theta^2},$$ (4.1)

which naturally suggests the poloidal ion gyroradius ρ_{θ_i} as the effective zonal flow screening length. Thus, in light of basic aspects of zonal flow physics [18,19], this implies that *the effective*
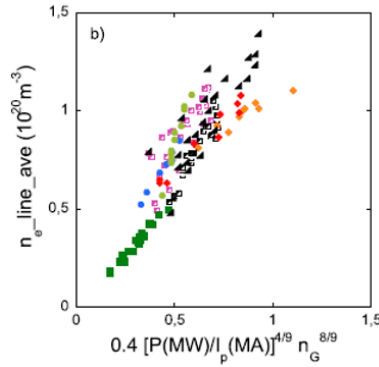
Figure 12. Scaling of density limit for L-mode experiments [8].

zonal flow inertia and screening length are lower for large I_p. Thus, for larger current, the shear layer will be concomitantly stronger, and more resilient against collapse at high density, suggesting a higher density limit. In this vein, shear layer physics and not $q(r)$, magnetic shear etc., is the underpinning of Greenwald scaling. This has interesting implications for stellarators, as well. Extending the Rosenbluth-Hinton theory, figure 13 illustrates the consequences for shear flow drive, in the context of zonal flow driven by incoherent mode coupling (drift wave beat noise). The key point is that higher current strengthens zonal flow shear, for fixed drive. Since the edge is

Figure 13. Connection between shear layer collapse and Greenwald scaling $\bar{n} \sim I_p$. Strong plasma current I_p can lower the neoclassical dielectric and then raise the zonal mode drive. As a result, shear flow becomes more robust and can sustain a higher density limit.

of primary interest in the context of density limits, we comment here that Singh and Diamond [35] also have shown that favorable I_p scaling of the asymptotic temporal response of the zonal potential persists in the plateau regime. In particular, the current scaling is the same, though the response is numerically smaller.

To extract a quantitative density limit scaling, one must combine:

— fluctuation and zonal flow evolution,
— neoclassical zonal flow screening,
— zonal flow damping (collisional),
— incoherent mode coupling and modulational instability.

These lead one to a new predator-prey model for turbulence-zonal flow evolution. Such a model was developed by Singh and Diamond (hereafter SD1) by extending previous versions of the predator-prey model. This model has features summarized in figure 14. Current scaling enters

Criterion for Shear Layer Collapse

- Derive shear layer persistence criterion

$$\frac{\rho_s}{(\rho_\theta L_n)^{\frac{1}{2}}} > \text{crit.}$$

$$\text{Crit} = \left[\frac{\eta}{\Omega_i} \frac{\gamma_d}{2k_{\hat{x}}^2 \rho_s^2 \Theta \Omega_i^2} \frac{\hat{\alpha}}{q_\perp^2 \rho_s^2} \frac{(1 + q_\perp^2 \rho_s^2)^3}{q_y^2 \rho_s^2} \right]^{1/4}$$

➔ Dimensionless parameter $\dfrac{\rho_s}{(\rho_\theta L_n)^{\frac{1}{2}}}$

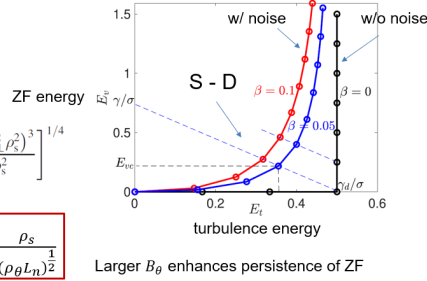Larger B_θ enhances persistence of ZF

Figure 14. Extended predator-prey model, yielding current scaling of the limiting density [35].

via zonal flow coupling (proportional to ϵ_{neo}^{-1}) and incoherent emission. These do not result from the linear growth rate, etc. Important developments in the analysis of the model are that the solution indicates zonal flow and turbulence always co-exist, though zonal energy can be weak. And the result that zonal flow energy increases with current, consistent with Greenwald scaling, enters via shear layer evolution. Inclusion of neoclassical zonal flow screening in the vein of the SD1 analysis recovers Greenwald scaling within the shear layer collapse paradigm.

Regarding stellarators, the implications of this theory are that the place to look for understanding of stellarator density limits is in edge zonal and shear flow physics and not magnetics, as is frequently assumed. Indeed, it is no surprise to learn that attempts to relate $\bar{n}_e$ scaling to iota, etc. have failed. A more promising road forward is to look at the scaling of the zonal flow screening length. For the case of the LHD stellarator, zonal flow screening is predicted to be essentially classical, with no neoclassical enhancement [60]. It's not entirely surprising then, that LHD has achieved very high densities [61].

The power scaling of the L-mode density limit is of interest, both in regards to the basic physics of the density limit and in the specific context of an improved confinement scenario of internal transport barrier (ITB) with an L-mode edge. Such a regime is a leading alternate plan for ITER, and is attractive, since it eliminates ELMs and other boundary-related complexities. A theory and model of the power dependence of the density limit follows, within the shear layer collapse paradigm. Existing understanding and modelling results developed to address the L $\rightarrow$ H transition are useful to this end. Recently, Singh and Diamond (SD2) [36] developed an extension of the Kim-Diamond model [9,14,62], of the L $\rightarrow$ H transition, and used this to investigate the evolution of zonal shears (as present in L-mode) at high density, with auxiliary power. SD2 solved coupled evolution equation for edge fluctuation energy $\mathcal{E}$, edge zonal shear energy v_z^2, edge density n and edge ion temperature gradient, written as $\mathcal{T}$ for simplicity. These equations are:

$$\frac{\partial \mathcal{E}}{\partial t} = \frac{a_1 \gamma(\mathcal{N}, \mathcal{T}) \mathcal{E}}{1 + a_3 \mathcal{V}^2} - a_2 \mathcal{E}^2 - \frac{a_4 v_z^2 \mathcal{E}}{1 + b_2 \mathcal{V}^2} \quad \text{(for fluctuation energy)} \tag{4.2a}$$

$$\frac{\partial v_z^2}{\partial t} = \frac{b_1 \mathcal{E} v_z^2}{1 + b_2 \mathcal{V}^2} - b_3 v_z^2 + b_4 \mathcal{E}^2 \quad \text{(for zonal flow energy)} \tag{4.2b}$$

$$\frac{\partial \mathcal{T}}{\partial t} = -c_1 \frac{\mathcal{E} \mathcal{T}}{1 + c_2 \mathcal{V}^2} - c_3 \mathcal{T} + Q \quad \text{(for edge } \nabla T_i) \tag{4.2c}$$

$$\frac{\partial n}{\partial t} = -d_1 \frac{\mathcal{E} n}{1 + d_2 \mathcal{V}^2} - d_3 n + S \quad \text{(for edge density)} \tag{4.2d}$$

Radial force balance gives the normalized mean $E \times B$ flow shear $\mathcal{V} \equiv V_E' a / \rho_* c_s$ as

$$\mathcal{V} \equiv \frac{V_E' a}{\rho_* c_s} = -\frac{n_0}{n} \mathcal{N} \left(\frac{n_0}{n} \mathcal{N} + \frac{T_0}{T} \mathcal{T} \right) \tag{4.3}$$

The model is zero dimensional. However, similar $L \to H$ models have been successfully extended to 1D [63,64], and such work is planned for the future. We note here that the SD2 model is simplified, and omits effects such as pressure curvature, toroidal velocity and mean poloidal velocity shear. These can induce asymmetries in the weighting of density and temperature gradients, which in turn affect the details of confinement regime transition dynamics. References [65,66] discuss this physics in detail, and its impact on the density limit power scaling will be a topic of future work. The SD2 model has been studied using the edge heat flux (Q) and the edge density source (e.g. fueling) variation. Here $Q = Q_i$, as it is ∇p_i which regulates $\langle E_r \rangle$—and thus the shear layer—via radial force balance. But note that for high density, $Q_i \approx Q_e$ is to be expected at the edge, regardless of the heating method. For simplicity, the model coefficients were specialized to the case of toroidal ITG turbulence. Scans of Q and edge density fueling source S were performed for 'L-mode' conditions (i.e. Q below criticality for the $L \to H$ transition). The principal goal was to explore the density dependence of the shear layer collapse. Results are given in figure 15, which shows the evolution of zonal flow energy (shear layer strength) vs time during Q(power) and S (fueling) variation. Note that zonal energy rises as Q is increased, flat-tops at
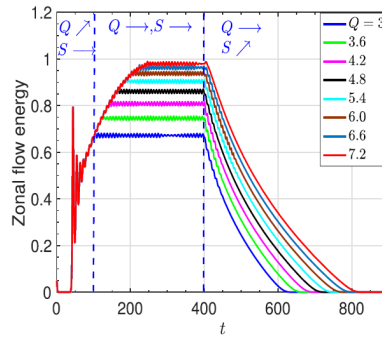

Figure 15. Evolution of zonal flow energy with various edge heat flux (Q) and edge density fueling source (S). Different colors refer to different power Q and ultimately to different shear layer collapse densities [36].

constant Q and then decays as S increases. The edge density increases with S (for fixed Q). *The values of S and n_{edge} for which v_z^2 vanishes clearly increase with Q, indicative of power scaling of shear layer collapse and thus of the L-mode density limit.* Oscillations in zonal energy during the Q-ramp are of the usual sort found in predator-prey systems. Defining the point of shear layer collapse as n_{crit} for which $v_z^2 \to 0$, the scaling of n_{crit} (and thus of the limiting density) with Q is seen to be $n_{crit} \sim Q^{1/3}$. Thus, shear layer physics leads naturally to power scaling. Explicit current scaling due to neoclassical ZF screening remains, i.e. $n_{crit} \sim I_p$, as in SD1. The power scaling obtained is distinct from Zanca's regression fit result, but is quite close (exponent of 0.33 vs 0.44)). Obviously, this model cannot address the distinction between n and $\bar{n}$, though there is ample evidence that these two are closely related. These results are limited to the case of ITG turbulence. However—as discussed above—such a model is relevant to high density L-mode edges at higher power. And it has the virtue of being comparatively insensitive to electron dissipation. Here, the key physics ultimately is the competition between drive via $\gamma(\nabla T)$ and zonal flow damping. And we should add there is a lot more information to be gleaned than that extracted from macroscopic scalings. But a careful surgical procedure is needed to expose the physics underlying the basic scans. To this end, consideration of the natural analogy between the $H \to L$ back-transition and the $L \to DL$ evolution suggests that hysteresis phenomena may be present in the dynamics of shear

layer collapse and the density limit. However, Caveat Emptor—the L $\to$ DL to H $\to$ L analogy is limited—even incorrect in some aspects—and must be used with care. That said, investigations of Q ramp-up $\to$ ramp-down evolution using the model of SD2 clearly manifest hysteresis in v_z^2 vs Q. These results are evident in figure 16, which shows both time evolution and a hysteresis loop in v_z^2 vs Q. It is important to note that this hysteresis is different from the usual sort. It is
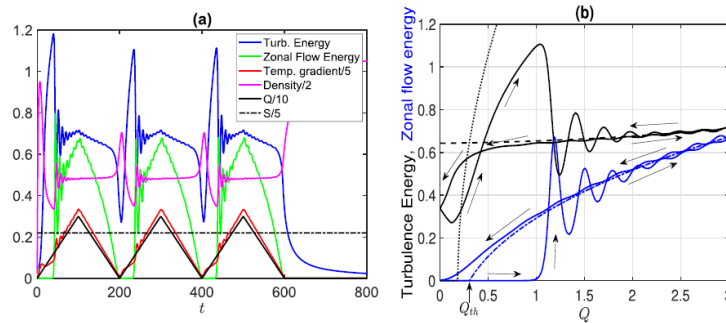

Figure 16. (a) Evolution of turbulence energy, zonal flow energy, temperature gradient and density during a cyclic ramp of input power Q. (b) Turbulence and Zonal flow hysteresis in a cyclic power ramp [36].

not due to bistability, since shear layer collapse, as modeled here, is a second order transition and hence does not involve bistability. Rather, the hysteresis here is due to the difference in temporal evolution between different state variables (i.e. different time delay rates). *Nevertheless, this result is likely of significant interest, as it links scaling to microscopics, and sets forth a clear, testable prediction of dynamics.* Further consideration of the H $\to$ L to L $\to$ DL analogy *begs the question of a possible torque dependence of the density limit*, distinct from power dependence?! This follows from shear layer physics, and the dependence of $\langle v_E \rangle'$ on $\langle v_\phi \rangle'$, via radial force balance.

5. H-mode Density Limit

The H-mode density limit [67–69] is manifested through a distinct compound phenomenology, involving:

— first, a H $\to$ L back transition at high density. This involves the decay of the mean $\langle E_r \rangle$ profile (primarily ∇p driven), and so is consistent with the shear layer collapse scenario;
— second, a rapid progression to $\bar{n}_G$, the limiting density. This is always the Greenwald value. At that point, disruptions frequently occur.

The H-mode density limit (HDL) is not nearly so thoroughly studied or understood as its L-mode counterpart is. The key question is the physics of the H $\to$ L back transition at high density. Once the back transition occurs, it's no surprise that enhanced transport, PTE's and edge cooling follow. This is unfortunate, since the fusion-relevant regime of high confinement at high power and high density will likely confront the HDL, rendering it a key issue for magnetic fusion. Mysteries abound in the lore of the HDL. For example, gentle pump-and-puff experiments have exceeded the Greenwald limit by a significant margin [70]. This is not surprising, since the edge $E \times B$ shear layer in H-mode is much stronger than its L-mode counterpart. Of course, the physics of the HDL is intimately connected to that of fueling and pedestal profile formation [71]. Candidate explanations of the HDL include ballooning instability at the separatrix [72]. The support for this is the apparent correlation of the HDL back-transition with the well known stability parameter α_{MHD}, evaluated at the separatrix. Fluctuation measurements supporting this suggestion are notably absent. Another scenario posits that at high density, the SOL particle dwell time is

determined by conduction, so $\tau_p \sim (Rq)^2/\chi_\parallel$, thus introducing density dependence to λ_{HD} via $\chi_\parallel$. Here $\lambda_{HD} \sim v_d \tau_p$ is the width of the SOL, as predicted by the Heuristic Drift (HD) model for H-mode [72]. The HD model has been broadly successful. Indeed, in the conduction regime, λ_{HD} *increases* with density (and collisionality). As λ_{HD} increases, $\langle v_E \rangle' \sim T_{sep}/\lambda_{HD}^2$ decreases. At sufficiently high density, then, shear stabilization in the SOL will be lost, and SOL interchange instability and turbulence should re-appear in H-mode. Brown and Goldston [73] hypothesize that the reappearance of SOL turbulence production may trigger the HDL, via, say, turbulence spreading from the SOL to the pedestal. They propose that this will degrade H-mode confinement and thus trigger a back-transition. Observe this is *an inward turbulence pulse propagation scenario*— a case where *'the tail wags the dog'*. A somewhat similar mechanism [55] has been suggested recently by other authors. Beyond the level of linear stability calculations, these scenarios are speculative. Experiments, including the requisite fluctuation studies, are sorely needed. Studies of macroscopics, alone, will not suffice. Theory and simulation work must address *dynamics*, too. Simulations here are especially difficult, since one must follow a full L $\rightarrow$ H transition cycle, with heat flux drive, fueling, and pedestal transport evolution. There are several interesting issues to address and the place for theory is evident.

6. Discussion and Summary

This paper has examined $E \times B$ shear $\langle v_E \rangle'$ as an 'order parameter' for the state of edge turbulence and transport in different regimes of toroidal confinement. H-mode, L-mode (including OH) and density limit (DL) regimes are considered, with special emphasis on the evolution from L $\rightarrow$ DL, i.e. the onset of density limit phenomenology. We submit that the three regimes may be classified by the edge shear condition according to:

(i) L-mode: *modest edge $E \times B$ shear*, both zonal and mean, which regulates turbulence.
(ii) H-mode: *strong pedestal $E \times B$ shear*, mostly mean flow driven by ∇p with significant turbulence suppression.
(iii) Density limit: *collapse of (L-mode) edge shear;* significant *increase* in edge turbulence, and PTE's, including turbulence spreading.

This classification builds upon our developing understanding of transport bifurcations and confinement transitions.

This paper focuses primarily upon the dynamics of L $\rightarrow$ DL evolution and the onset of density limit phenomenology. It features and describes the shear layer collapse paradigm and its relation to increased levels of PTE's. The theory of the edge shear layer paradigm depends heavily upon the basic theory of zonal flow evolution, and predator-prey system dynamics. Our understanding of the physics of spreading and other PTE's is still developing, and needs to be reconciled with the theory of zonal flows.

Several clear trends and ideas can be distilled from the body of work on transport physics of density limits in L-mode. First, edge shear layer decay and collapse are observed as the line-averaged density $\bar{n}_e$ approaches the Greenwald density, i.e. $\bar{n}_e \rightarrow \bar{n}_G$. Reynolds power drops while the particle flux increases. Turbulence spreading and PTE's are observed to increase. In one case, the rise in spreading power is comparable to the drop in Reynolds power. Electron adiabaticity $\alpha = k_\parallel^2 v_{the}^2/\omega \nu_{e,e}$ emerges as a key parameter. In particular, the rise in particle flux and drop in Reynolds power are correlated with the drop in α as $\bar{n}_e \rightarrow \bar{n}_G$. This is consistent with our understanding of the decline in zonal flow production for hydrodynamic electrons. However, while α is surely a key parameter, it does not necessarily indicate *causality*. In particular, a recent study of the hysteresis of α with respect to $\langle v_E \rangle'$ variation during bias experiments suggests that α may actually "follow" $\langle v_E \rangle'$. Further study of this important question is needed.

The relevant scalings for L $\rightarrow$ DL evolution are related to plasma current—i.e. the familiar Greenwald scaling $\bar{n}_G \sim I_p/a^2$, and the re-emerging scaling of the limiting density with power. Zonal flow physics reconciles the shear layer collapse scenario with both of these observed

trends. Current scaling has been shown to emerge from the neoclassical dielectric screening of the zonal flow—i.e. stronger screening $B_\theta \rightarrow$ smaller effective inertia of zonal flows $\rightarrow$ larger zonal flow shear $\rightarrow$ a more robust shear layer and thus a larger edge density and ultimately a higher density limit. Similarly, power scaling enters via Reynolds stress and its competition with zonal flow damping. Increased power $\rightarrow$ implies increased fluctuation levels driving a larger Reynolds power which yields a stronger L-mode flow shear and so a larger limiting density. Theory recovers $\bar{n}_e \sim I_p$ for fixed power, and $\bar{n}_e \sim I_p^2 Q_i^{1/3}$ for scaling with variable edge ion heat flux (i.e. power). These scalings predict the edge density scaling. The connection to $\bar{n}_e$ has yet to be fully determined. Theory predicts a novel sort of hysteresis in n_e vs Q_i. Such hysteresis is dynamical, and due to a delay in zonal flow evolution on account of critical slowing down. This prediction constitutes a link between the microscopics and macroscopics of density limits. Physics based scaling trends and their understanding are only just emerging, and considerable research lies ahead.

Future experimental work should focus on:

— causality—i.e. can shear layer collapse be shown to be the trigger for a density limit disruption? Here, the temporal sequence of collapse, spreading, radiation, and MHD activity must be demonstrated. How do the candidate key parameters α, $\langle v_E \rangle' / \Delta\omega_{\vec{k}}$ (shearing rate normalized to decorrelation rate) evolve during shear layer collapse?
— *current and power ramp experiments*. Current should be ramped down at fixed density, to probe density limit causality, and power should be ramped up and down, to examine hysteresis. Fluctuation measurements are essential to both studies. Current ramps are a promising and under-utilized probe of edge and SOL turbulence.
— *slow bias probe ramp up and down*, to further explore causality vs correlation in the relation of edge shears to adiabaticity.
— *studies of* core-SOL coupling, *turbulence spreading*, and the time sequence of evolution near the HDL.
— Comparative studies of the density limit physics in negative and positive triangularity plasmas, and the relation to differences in edge shear layer and turbulence between these two configurations.

Future theoretical work should: focus on *1D models*. This is especially important for causality studies. Collisionless regimes are also highly relevant, and largely untouched in the context of density limits. *Short wavelength ∇n-driven CTEMs and the associated zonal modes* are elements of a quite promising direction. The aim here is to move beyond the 'adiabaticity-as-key-parameter' paradigm.

Here, we also suggest some speculative directions for future research. These include:

— Does SOL $\rightarrow$ edge turbulence invasion account for the HDL? Does the pedestal cool and exhibit degraded confinement as the HDL is approached? Do these occur independent of SOL $\rightarrow$ pedestal turbulence invasion? How much is the HDL due to pedestal decay vs SOL physics?
— Can means such as the NTV (Neoclassical Toroidal Viscosity), be used to enhance edge density and 'beat' the density limit? NTV has been used to lower the L $\rightarrow$ H threshold [74]. Early results from electrode bias experiments suggest an answer in the affirmative.
— Can the increased power $\rightarrow$ higher density $\rightarrow$ higher fusion gain $\rightarrow$ higher power... *feedback loop actually be realized, controlled, and exploited in an I-mode edge*? What new plasma regimes will be encountered?

And finally:

— Does a DL-L-H coexistence 'triple point' of confinement regimes exist, in analogy to phase coexistence triple points? Up to now, it appears that a H $\rightarrow$ L back transition always

occurs prior to arriving at the density limit (i.e. two phase coexistence, only). Will this trend persist?

All told, many interesting questions concerning the transport physics of the density limit remain to be explored and answered.

7. Conclusion

In this 'perspective' paper, we have surveyed the states of the tokamak edge plasma, and identified the edge electric field shear $\langle v_E \rangle'$, as a natural order parameter. Special emphasis was placed on plasmas at the density limit, in which the edge is strongly turbulent, with weak shearing effects. The many lessons learned from 40 years of H-mode study were exploited in a new context. The (near) density limit regime was characterized as a distinct confinement state 'phase', and the L $\rightarrow$ DL evolution emerged as a type of confinement phase transition. The shear layer collapse paradigm was presented and discussed in detail, along with its (causal) relation to enhanced particle transport events (PTE's), which are observed in density limit regimes. The status of the theory of density limit scalings with current (edge B_θ) and power (edge Q_i) was presented. The connections between density limit physics and fundamental ideas from L $\rightarrow$ H theory were emphasized throughout.

Future work will likely focus on the H-mode density limit—an H $\rightarrow$ L back transition problem par excellence, and one which is crucial to magnetic fusion. Another important direction is to address the relation of density limits to detachment, and the roles of the SOL and the divertor in density limit physics. Intermittency (i.e. 'blob' and their statistics) and its relation to density limit dynamics (i.e. cause or effect?) is yet another interesting question. Last but not least, theory must produce testable predictions of the key dimensionless parameters (N.B.: There are several!) which characterize density limit physics.

Many interesting problems remain. We can look forward to many more in the fast approaching age of burning plasmas. And the utility of ideas and approaches from L $\rightarrow$ H transition physics is a testament to the enduring impact of the discovery of the H-mode, 40 years ago.

A. Singh-Diamond Model 2

The Singh-Diamond Model 2 [36] (equation (4.2) and equation (4.3)) is a zero dimensional model evolving turbulence energy $\mathcal{E} = q_y^2 \rho_s^2 I_q / q_y^2 \rho_s^2 \rho_*^2$, zonal flow energy v_z^2, mean temperature gradient ∇T ($\mathcal{T}$), and mean density n. In this model, time is normalized by the gyro-Bohm diffusion time, i.e., $t \equiv t D_{GB}/a^2$, where $D_{GB} = c_i \rho_i \rho_*$ is the gyro-Bohm diffusivity, a is the minor radius. Subscripts $\vec{q}$ and $\vec{k}$ represent the wave vector of zonal flow and turbulence modes, respectively. Definitions for the quantities and coefficients of equation (4.2) and equation (4.3) are as follows: $\mathcal{T} = -a\nabla T/T_0$ and $\mathcal{N} = -a\nabla n/n_0$ are normalized temperature and density gradients; $a_1 \equiv a_1 a/c_i \rho_*^2$ is the normalized growth rate coefficient; $a_2 \equiv a_2 a/c_i \rho_*^2$ is the normalized nonlinear damping rate; factor $1/(1 + a_3 \mathcal{V})$ is the growth rate reduction by mean flow shear $\mathcal{V}$; $a_4 = b_1 = 2(k_x^2 \rho_s^2/\varepsilon \rho_*^2) \left(\sum_q \Theta_{k,-q,q} c_s/a \right)$ is the coefficient of the modulational growth of zonal flow by

Reynolds stress, where Θ is the triad interaction time, and $\varepsilon \sim I_p^2$; factor $1/(1 + b_2 \mathcal{V}^2)$ is the growth rate reduction of the zonal flow by the mean flow shear; b_3 is the coefficient of the collisional damping of the zonal flow; $b_4 = (4/\varepsilon \rho_*^2) \sum_q q_x^2 \rho_s^2 q_y^2 \rho_s^2 \Theta(c_s/a)$ is the zonal noise, which is a unique feature of the SD2 Model; $c_1 = (a/L)^2 (\chi_T/D_{GB})$ and $c_3 = (a/L)^2 (\chi_{nc}/D_{GB})$ are coefficients of the local turbulent damping and neoclassical damping, where χ_T and χ_{nc} are turbulent and neoclassical heat diffusivities, and L is the impurity radiation power loss; factor $1/(1 + c_2 \mathcal{V}^2)$ is the transport suppression due to cross-phase reduction by the mean flow shear; $Q = a^2 \nabla S_T / T_0 c_i \rho_*^2$ is the normalized source function representing the input external power, where S_T is the actual source function; $d_1 = (a/L)^2 (D_T/D_{GB})$ and $d_3 = (a/L)^2 (D_{nc}/D_{GB})$ are normalized turbulent and neoclassical damping coefficients, where D_T and D_{nc} are turbulent and neoclassical particle diffusivities; factor $1/(1 + d_2 \mathcal{V}^2)$ is the transport suppression due to cross-phase reduction by the mean flow shear; $S = aS_n / n_0 c_i \rho^{*2}$ is the normalized particle source function, where S_n is the actual particle source function; $\mathcal{V}$ is the normalized mean flow shear.

References

1. F. Wagner, G. Becker, K. Behringer, D. Campbell, A. Eberhagen *et al.*, "Regime of improved confinement and high beta in neutral-beam-heated divertor discharges of the asdex tokamak," *Phys. Rev. Lett.*, vol. 49, pp. 1408–1412, Nov 1982. [Online]. Available: https://link.aps.org/doi/10.1103/PhysRevLett.49.1408

2. M. Greenwald, J. Terry, S. Wolfe, S. Ejima, M. Bell, S. Kaye, and G. Neilson, "A new look at density limits in tokamaks," *Nuclear Fusion*, vol. 28, no. 12, pp. 2199–2207, dec 1988. [Online]. Available: https://doi.org/10.1088/0029-5515/28/12/009

3. J. W. Connor and H. R. Wilson, "A review of theories of the l-h transition," *Plasma Physics and Controlled Fusion*, vol. 42, no. 1, pp. R1–R74, dec 1999. [Online]. Available: https://doi.org/10.1088/0741-3335/42/1/201

4. F. Wagner, "A quarter-century of h-mode studies," *Plasma Physics and Controlled Fusion*, vol. 49, no. 12B, pp. B1–B33, nov 2007. [Online]. Available: https://doi.org/10.1088/0741-3335/49/12b/s01

5. R. Hong, G. Tynan, P. Diamond, L. Nie, D. Guo, T. Long, R. Ke, Y. Wu, B. Yuan, and M. X. and, "Edge shear flows and particle transport near the density limit of the HL-2a tokamak," *Nuclear Fusion*, vol. 58, no. 1, p. 016041, dec 2017. [Online]. Available: https://doi.org/10.1088/1741-4326/aa9626

6. M. Greenwald, "Density limits in toroidal plasmas," *Plasma Physics and Controlled Fusion*, vol. 44, no. 8, pp. R27–R53, jul 2002. [Online]. Available: https://doi.org/10.1088/0741-3335/44/8/201

7. M. Greenwald, A. Bader, S. Baek, M. Bakhtiari, H. Barnard, W. Beck, W. Bergerson, I. Bespamyatnov, P. Bonoli, D. Brower *et al.*, "20 years of research on the alcator c-mod tokamak," *Physics of Plasmas*, vol. 21, no. 11, p. 110501, 2014. [Online]. Available: https://doi.org/10.1063/1.4901920

8. P. Zanca, F. Sattin, and D. E. and, "A power-balance model of the density limit in fusion plasmas: application to the l-mode tokamak," *Nuclear Fusion*, vol. 59, no. 12, p. 126011, sep 2019. [Online]. Available: https://doi.org/10.1088/1741-4326/ab3b31

9. P. H. Diamond, Y.-M. Liang, B. A. Carreras, and P. W. Terry, "Self-regulating shear flow turbulence: A paradigm for the l to h transition," *Phys. Rev. Lett.*, vol. 72, pp. 2565–2568, Apr 1994. [Online]. Available: https://link.aps.org/doi/10.1103/PhysRevLett.72.2565

10. E.-j. Kim and P. H. Diamond, "Zonal flows and transient dynamics of the $l-h$ transition," *Phys. Rev. Lett.*, vol. 90, p. 185006, May 2003. [Online]. Available: https://link.aps.org/doi/10.1103/PhysRevLett.90.185006

11. R. J. Goldston, "Energy confinement scaling in tokamaks: some implications of recent experiments with ohmic and strong auxiliary heating," *Plasma Physics and Controlled Fusion*, vol. 26, no. 1A, pp. 87–103, jan 1984. [Online]. Available: https://doi.org/10.1088/0741-3335/26/1a/308

12. Y. Koide, M. Kikuchi, M. Mori, S. Tsuji, S. Ishida, N. Asakura, Y. Kamada, T. Nishitani, Y. Kawano, T. Hatae, T. Fujita, T. Fukuda, A. Sakasai, T. Kondoh, R. Yoshino, and Y. Neyatani, "Internal transport barrier on q=3 surface and poloidal plasma spin up in jt-60u

high-β_p discharges," *Phys. Rev. Lett.*, vol. 72, pp. 3662–3665, Jun 1994. [Online]. Available: https://link.aps.org/doi/10.1103/PhysRevLett.72.3662

13. F. L. Hinton, "Thermal confinement bifurcation and the l- to h-mode transition in tokamaks," *Physics of Fluids B: Plasma Physics*, vol. 3, no. 3, pp. 696–704, 1991. [Online]. Available: https://doi.org/10.1063/1.859866

14. V. B. Lebedev and P. H. Diamond, "Theory of the spatiotemporal dynamics of transport bifurcations," *Physics of Plasmas*, vol. 4, no. 4, pp. 1087–1096, 1997. [Online]. Available: https://doi.org/10.1063/1.872196

15. H. Biglari, P. H. Diamond, and P. W. Terry, "Influence of sheared poloidal rotation on edge turbulence," *Physics of Fluids B: Plasma Physics*, vol. 2, no. 1, pp. 1–4, 1990. [Online]. Available: https://doi.org/10.1063/1.859529

16. K. H. Burrell, "Effects of e×b velocity shear and magnetic shear on turbulence and transport in magnetic confinement devices," *Physics of Plasmas*, vol. 4, no. 5, pp. 1499–1518, 1997. [Online]. Available: https://doi.org/10.1063/1.872367

17. R. A. Heinonen and P. H. Diamond, "Subcritical turbulence spreading and avalanche birth," *Physics of Plasmas*, vol. 26, no. 3, p. 030701, 2019. [Online]. Available: https://doi.org/10.1063/1.5083176

18. P. H. Diamond, S.-I. Itoh, K. Itoh, and T. S. Hahm, "Zonal flows in plasma—a review," *Plasma Physics and Controlled Fusion*, vol. 47, no. 5, pp. R35–R161, apr 2005. [Online]. Available: https://doi.org/10.1088/0741-3335/47/5/r01

19. O. D. Gurcan and P. H. Diamond, "Zonal flows and pattern formation," *Journal of Physics A: Mathematical and Theoretical*, vol. 48, no. 29, p. 293001, jul 2015. [Online]. Available: https://doi.org/10.1088/1751-8113/48/29/293001

20. D. G. Dritschel and M. E. McIntyre, "Multiple jets as pv staircases: The phillips effect and the resilience of eddy-transport barriers," *Journal of the Atmospheric Sciences*, vol. 65, no. 3, pp. 855 – 874, 2008. [Online]. Available: https://doi.org/10.1175/2007JAS2227.1

21. X. Wang, H.-Y. Shih, and N. Goldenfeld, "Stochastic model for quasi-one-dimensional transitional turbulence with streamwise shear interactions," *Phys. Rev. Lett.*, vol. 129, p. 034501, Jul 2022. [Online]. Available: https://link.aps.org/doi/10.1103/PhysRevLett.129.034501

22. L. Schmitz, L. Zeng, T. L. Rhodes, J. C. Hillesheim, E. J. Doyle, R. J. Groebner, W. A. Peebles, K. H. Burrell, and G. Wang, "Role of zonal flow predator-prey oscillations in triggering the transition to h-mode confinement," *Phys. Rev. Lett.*, vol. 108, p. 155002, Apr 2012. [Online]. Available: https://link.aps.org/doi/10.1103/PhysRevLett.108.155002

23. K. Miki, P. Diamond, N. Fedorczak, O. Gurcan, M. Malkov, C. Lee, Y. Kosuga, G. Tynan, G. Xu, T. Estrada, D. McDonald, L. Schmitz, and K. Zhao, "Spatio-temporal evolution of the l → h and h → l transitions," *Nuclear Fusion*, vol. 53, no. 7, p. 073044, jun 2013. [Online]. Available: https://doi.org/10.1088/0029-5515/53/7/073044

24. H. R. Wilson, J. W. Connor, A. R. Field, S. J. Fielding, R. L. Miller, L. L. Lao, J. R. Ferron, and A. D. Turnbull, "Ideal magnetohydrodynamic stability of the tokamak high-confinement-mode edge region," *Physics of Plasmas*, vol. 6, no. 5, pp. 1925–1934, 1999. [Online]. Available: https://doi.org/10.1063/1.873492

25. K. Burrell, A. Garofalo, W. Solomon, M. Fenstermacher, D. Orlov, T. Osborne, J.-K. Park, and P. Snyder, "Quiescent h-mode operation using torque from non-axisymmetric, non-resonant magnetic fields," *Nuclear Fusion*, vol. 53, no. 7, p. 073038, jun 2013. [Online]. Available: https://doi.org/10.1088/0029-5515/53/7/073038

26. D. Whyte, A. Hubbard, J. Hughes, B. Lipschultz, J. Rice, E. Marmar, M. Greenwald, I. Cziegler, A. Dominguez, T. Golfinopoulos, N. Howard, L. Lin, R. McDermott, M. Porkolab, M. Reinke, J. Terry, N. Tsujii, S. Wolfe, S. Wukitch, and Y. L. and, "I-mode: an h-mode energy confinement regime with l-mode particle transport in alcator c-mod," *Nuclear Fusion*, vol. 50, no. 10, p. 105005, aug 2010. [Online]. Available: https://doi.org/10.1088/0029-5515/50/10/105005

27. X. Chen, K. Burrell, T. Osborne, K. Barada, N. Ferraro, A. Garofalo, R. Groebner, G. McKee, C. Petty, M. Porkolab, T. Rhodes, J. Rost, P. Snyder, W. Solomon, and Z. Y. and, "Bifurcation of quiescent h-mode to a wide pedestal regime in DIII-d and advances in the understanding of edge harmonic oscillations," *Nuclear Fusion*, vol. 57, no. 8, p. 086008, jun 2017. [Online]. Available: https://doi.org/10.1088/1741-4326/aa7531

28. T. Evans, R. Moyer, J. Watkins, P. Thomas, T. Osborne, J. Boedo, M. Fenstermacher, K. Finken, R. Groebner, M. Groth, J. Harris, G. Jackson, R. L. Haye, C. Lasnier, M. Schaffer, G. Wang, and

20

rsta.royalsocietypublishing.org   Phil. Trans. R. Soc. A 0000000

L. Zeng, "Suppression of large edge localized modes in high confinement diii-d plasmas with a stochastic magnetic boundary," *Journal of Nuclear Materials*, vol. 337-339, pp. 691–696, 2005, pSI-16. [Online]. Available: https://doi.org/10.1016/j.jnucmat.2004.10.062

29. M. Kikuchi, T. Takizuka, S. Medvedev, T. Ando, D. Chen, J. Li, M. Austin, O. Sauter, L. Villard, A. Merle, M. Fontana, Y. Kishimoto, and K. Imadera, "L-mode-edge negative triangularity tokamak reactor," *Nuclear Fusion*, vol. 59, no. 5, p. 056017, apr 2019. [Online]. Available: https://doi.org/10.1088/1741-4326/ab076d

30. D. A. Gates and L. Delgado-Aparicio, "Origin of tokamak density limit scalings," *Phys. Rev. Lett.*, vol. 108, p. 165004, Apr 2012. [Online]. Available: https://link.aps.org/doi/10.1103/PhysRevLett.108.165004

31. B. LaBombard, R. L. Boivin, M. Greenwald, J. Hughes, B. Lipschultz, D. Mossessian, C. S. Pitcher, J. L. Terry, and S. J. Zweben, "Particle transport in the scrape-off layer and its relationship to discharge density limit in alcator c-mod," *Physics of Plasmas*, vol. 8, no. 5, pp. 2107–2117, 2001. [Online]. Available: https://doi.org/10.1063/1.1352596

32. Y. Xu, D. Carralero, C. Hidalgo, S. Jachmich, P. Manz, E. Martines, B. van Milligen, M. Pedrosa, M. Ramisch, I. Shesterikov, C. Silva, M. Spolaore, U. Stroth, and N. Vianello, "Long-range correlations and edge transport bifurcation in fusion plasmas," *Nuclear Fusion*, vol. 51, no. 6, p. 063020, may 2011. [Online]. Available: https://doi.org/10.1088/0029-5515/51/6/063020

33. B. N. Rogers, J. F. Drake, and A. Zeiler, "Phase space of tokamak edge turbulence, the $L - H$ transition, and the formation of the edge pedestal," *Phys. Rev. Lett.*, vol. 81, pp. 4396–4399, Nov 1998. [Online]. Available: https://link.aps.org/doi/10.1103/PhysRevLett.81.4396

34. R. J. Hajjar, P. H. Diamond, and M. A. Malkov, "Dynamics of zonal shear collapse with hydrodynamic electrons," *Physics of Plasmas*, vol. 25, no. 6, p. 062306, 2018. [Online]. Available: https://doi.org/10.1063/1.5030345

35. R. Singh and P. Diamond, "Bounds on edge shear layer persistence while approaching the density limit," *Nuclear Fusion*, vol. 61, no. 7, p. 076009, jun 2021. [Online]. Available: https://doi.org/10.1088/1741-4326/abfadb

36. R. Singh and P. H. Diamond, "Zonal shear layer collapse and the power scaling of the density limit: old l-h wine in new bottles," *Plasma Physics and Controlled Fusion*, vol. 64, no. 8, p. 084004, jul 2022. [Online]. Available: https://doi.org/10.1088/1361-6587/ac7972

37. B. Lipschultz, B. LaBombard, E. Marmar, M. Pickrell, J. Terry, R. Watterson, and S. Wolfe, "Marfe: an edge plasma phenomenon," *Nuclear Fusion*, vol. 24, no. 8, pp. 977–988, aug 1984. [Online]. Available: https://doi.org/10.1088/0029-5515/24/8/002

38. C. P. Ritz, H. Lin, T. L. Rhodes, and A. J. Wootton, "Evidence for confinement improvement by velocity-shear suppression of edge turbulence," *Phys. Rev. Lett.*, vol. 65, pp. 2543–2546, Nov 1990. [Online]. Available: https://link.aps.org/doi/10.1103/PhysRevLett.65.2543

39. C. Hidalgo, M. A. Pedrosa, E. Sánchez, R. Balbín, A. López-Fraguas, B. van Milligen, C. Silva, H. Fernandes, C. A. F. Varandas, C. Riccardi, R. Carrozza, M. Fontanesi, B. A. Carreras, and L. García, "Generation of sheared poloidal flows via reynolds stress and transport barrier physics," *Plasma Physics and Controlled Fusion*, vol. 42, no. 5A, pp. A153–A160, may 2000. [Online]. Available: https://doi.org/10.1088/0741-3335/42/5a/316

40. C. Hidalgo, M. A. Pedrosa, L. García, and A. Ware, "Experimental evidence of coupling between sheared-flow development and an increase in the level of turbulence in the TJ−II stellarator," *Phys. Rev. E*, vol. 70, p. 067402, Dec 2004. [Online]. Available: https://link.aps.org/doi/10.1103/PhysRevE.70.067402

41. T. Long, P. Diamond, R. Ke, L. Nie, M. Xu, X. Zhang, B. Li, Z. Chen, X. Xu, Z. Wang, T. Wu, W. Tian, J. Yuan, B. Yuan, S. Gong, C. Xiao, J. Gao, Z. Hao, N. Wang, Z. Chen, Z. Yang, L. Gao, Y. Ding, Y. Pan, W. Chen, G. Hao, J. Li, W. Zhong, and X. Duan, "Enhanced particle transport events approaching the density limit of the j-TEXT tokamak," *Nuclear Fusion*, vol. 61, no. 12, p. 126066, nov 2021. [Online]. Available: https://doi.org/10.1088/1741-4326/ac36f2

42. T. Eich, P. Manz, and the ASDEX Upgrade team, "The separatrix operational space of ASDEX upgrade due to interchange-drift-alfvén turbulence," *Nuclear Fusion*, vol. 61, no. 8, p. 086017, jul 2021. [Online]. Available: https://doi.org/10.1088/1741-4326/ac0412

43. R. Numata, R. Ball, and R. L. Dewar, "Bifurcation in electrostatic resistive drift wave turbulence," *Physics of Plasmas*, vol. 14, no. 10, p. 102312, 2007. [Online]. Available: https://doi.org/10.1063/1.2796106

44. K. Ghantous and O. D. Gürcan, "Wave-number spectrum of dissipative drift waves and a transition scale," *Phys. Rev. E*, vol. 92, p. 033107, Sep 2015. [Online]. Available: https://link.aps.org/doi/10.1103/PhysRevE.92.033107

45. P. Manz, T. T. Ribeiro, B. D. Scott, G. Birkenmeier, D. Carralero, G. Fuchert, S. H. Müller, H. W. Müller, U. Stroth, and E. Wolfrum, "Origin and turbulence spreading of plasma blobs," *Physics of Plasmas*, vol. 22, no. 2, p. 022308, 2015. [Online]. Available: https://doi.org/10.1063/1.4908272

46. P. H. Diamond and T. S. Hahm, "On the dynamics of turbulent transport near marginal stability," *Physics of Plasmas*, vol. 2, no. 10, pp. 3640–3649, 1995. [Online]. Available: https://doi.org/10.1063/1.871063

47. J. A. Boedo, D. L. Rudakov, R. A. Moyer, G. R. McKee, R. J. Colchin, M. J. Schaffer, P. G. Stangeby, W. P. West, S. L. Allen, T. E. Evans, R. J. Fonck, E. M. Hollmann, S. Krasheninnikov, A. W. Leonard, W. Nevins, M. A. Mahdavi, G. D. Porter, G. R. Tynan, D. G. Whyte, and X. Xu, "Transport by intermittency in the boundary of the diii-d tokamak," *Physics of Plasmas*, vol. 10, no. 5, pp. 1670–1677, 2003. [Online]. Available: https://doi.org/10.1063/1.1563259

48. G. Grenfell, B. van Milligen, U. Losada, W. Ting, B. Liu, C. Silva, M. Spolaore, and C. H. and, "Measurement and control of turbulence spreading in the scrape-off layer of TJ-II stellarator," *Nuclear Fusion*, vol. 59, no. 1, p. 016018, dec 2018. [Online]. Available: https://doi.org/10.1088/1741-4326/aaf034

49. K. Miki, P. H. Diamond, L. Schmitz, D. C. McDonald, T. Estrada, O. D. Gurcan, and G. R. Tynan, "Spatio-temporal evolution of the h → l back transition," *Physics of Plasmas*, vol. 20, no. 6, p. 062304, 2013. [Online]. Available: https://doi.org/10.1063/1.4812555

50. R. Ke, P. Diamond, T. Long, M. Xu, Z. Chen, L. Gao, Q. Yang, Y. Wang, X. Zhang, L. Nie, T. Wu, J. Gao, D. Li, N. Wang, Z. Yang, Z. Chen, Y. Pan, and X. Duan, "Electrode biasing maintains the edge shear layer at high density in the j-TEXT tokamak," *Nuclear Fusion*, vol. 62, no. 7, p. 076014, may 2022. [Online]. Available: https://doi.org/10.1088/1741-4326/ac5fe9

51. R. J. Taylor, M. L. Brown, B. D. Fried, H. Grote, J. R. Liberati, G. J. Morales, P. Pribyl, D. Darrow, and M. Ono, "H-mode behavior induced by cross-field currents in a tokamak," *Phys. Rev. Lett.*, vol. 63, pp. 2365–2368, Nov 1989. [Online]. Available: https://link.aps.org/doi/10.1103/PhysRevLett.63.2365

52. G. R. Tynan, L. Schmitz, R. W. Conn, R. Doerner, and R. Lehmer, "Steady-state convection and fluctuation-driven particle transport in the h-mode transition," *Phys. Rev. Lett.*, vol. 68, pp. 3032–3035, May 1992. [Online]. Available: https://link.aps.org/doi/10.1103/PhysRevLett.68.3032

53. I. Shesterikov, Y. Xu, G. R. Tynan, P. H. Diamond, S. Jachmich, P. Dumortier, M. Vergote, M. Van Schoor, G. Van Oost, and T. Team, "Experimental evidence for the intimate interaction among sheared flows, eddy structures, reynolds stress, and zonal flows across a transition to improved confinement," *Phys. Rev. Lett.*, vol. 111, p. 055006, Aug 2013. [Online]. Available: https://link.aps.org/doi/10.1103/PhysRevLett.111.055006

54. M. Giacomin and P. Ricci, "Investigation of turbulent transport regimes in the tokamak edge by using two-fluid simulations," *Journal of Plasma Physics*, vol. 86, no. 5, p. 905860502, 2020.

55. M. Giacomin, A. Pau, P. Ricci, O. Sauter, T. Eich, the ASDEX Upgrade team, J. Contributors, and the TCV team, "First-principles density limit scaling in tokamaks based on edge turbulent transport and implications for iter," *Phys. Rev. Lett.*, vol. 128, p. 185003, May 2022. [Online]. Available: https://link.aps.org/doi/10.1103/PhysRevLett.128.185003

56. T. Rhodes, C. Ritz, and R. Bengtson, "Scaling of far edge plasma turbulence and fluctuation induced particle transport in the TEXT tokamak," *Nuclear Fusion*, vol. 33, no. 8, pp. 1147–1163, aug 1993. [Online]. Available: https://doi.org/10.1088/0029-5515/33/8/i05

57. M. N. Rosenbluth and F. L. Hinton, "Poloidal flow driven by ion-temperature-gradient turbulence in tokamaks," *Phys. Rev. Lett.*, vol. 80, pp. 724–727, Jan 1998. [Online]. Available: https://link.aps.org/doi/10.1103/PhysRevLett.80.724

58. R. Singh and P. H. Diamond, "A unified theory of zonal flow shears and density corrugations in drift wave turbulence," *Plasma Physics and Controlled Fusion*, vol. 63, no. 3, p. 035015, jan 2021. [Online]. Available: https://doi.org/10.1088/1361-6587/abd618

59. F. L. Hinton and J. A. Robertson, "Neoclassical dielectric property of a tokamak plasma," *The Physics of Fluids*, vol. 27, no. 5, pp. 1243–1247, 1984. [Online]. Available: https://aip.scitation.org/doi/abs/10.1063/1.864478

60. H. Sugama and T.-H. Watanabe, "Dynamics of zonal flows in helical systems," *Phys. Rev. Lett.*, vol. 94, p. 115001, Mar 2005. [Online]. Available: https://link.aps.org/doi/10.1103/PhysRevLett.94.115001

61. N. Ohyabu, T. Morisaki, S. Masuzaki, R. Sakamoto, M. Kobayashi, J. Miyazawa, M. Shoji, A. Komori, and O. Motojima, "Observation of stable superdense core plasmas in the

large helical device," *Phys. Rev. Lett.*, vol. 97, p. 055002, Aug 2006. [Online]. Available: https://link.aps.org/doi/10.1103/PhysRevLett.97.055002

62. E.-j. Kim and P. H. Diamond, "Zonal flows and transient dynamics of the $l-h$ transition," *Phys. Rev. Lett.*, vol. 90, p. 185006, May 2003. [Online]. Available: https://link.aps.org/doi/10.1103/PhysRevLett.90.185006

63. K. Miki, P. H. Diamond, O. D. Gurcan, G. R. Tynan, T. Estrada, L. Schmitz, and G. S. Xu, "Spatio-temporal evolution of the l→i→h transition," *Physics of Plasmas*, vol. 19, no. 9, p. 092306, 2012. [Online]. Available: https://doi.org/10.1063/1.4753931

64. M. A. Malkov, P. H. Diamond, K. Miki, J. E. Rice, and G. R. Tynan, "Linking the micro and macro: L-h transition dynamics and threshold physics," *Physics of Plasmas*, vol. 22, no. 3, p. 032506, 2015. [Online]. Available: https://doi.org/10.1063/1.4914934

65. L. Chôné, P. Beyer, Y. Sarazin, G. Fuhr, C. Bourdelle, and S. Benkadda, "L-h transition dynamics in fluid turbulence simulations with neoclassical force balance," *Physics of Plasmas*, vol. 21, no. 7, p. 070702, 2014. [Online]. Available: https://doi.org/10.1063/1.4890971

66. ——, "Mechanisms and dynamics of the external transport barrier formation in non-linear plasma edge simulations," *Nuclear Fusion*, vol. 55, no. 7, p. 073010, jun 2015. [Online]. Available: https://dx.doi.org/10.1088/0029-5515/55/7/073010

67. R. Goldston, "Theoretical aspects and practical implications of the heuristic drift sol model," *Journal of Nuclear Materials*, vol. 463, pp. 397–400, 2015, pLASMA-SURFACE INTERACTIONS 21. [Online]. Available: https://doi.org/10.1016/j.jnucmat.2014.10.080

68. T. Eich, R. Goldston, A. Kallenbach, B. Sieglin, H. Sun, and and, "Correlation of the tokamak h-mode density limit with ballooning stability at the separatrix," *Nuclear Fusion*, vol. 58, no. 3, p. 034001, jan 2018. [Online]. Available: https://doi.org/10.1088/1741-4326/aaa340

69. M. Bernert, T. Eich, A. Kallenbach, D. Carralero, A. Huber, P. T. Lang, S. Potzel, F. Reimold, J. Schweinzer, E. Viezzer, and H. Zohm, "The h-mode density limit in the full tungsten ASDEX upgrade tokamak," *Plasma Physics and Controlled Fusion*, vol. 57, no. 1, p. 014038, nov 2014. [Online]. Available: https://doi.org/10.1088/0741-3335/57/1/014038

70. T. H. Osborne, A. W. Leonard, M. A. Mahdavi, M. Chu, M. E. Fenstermacher, R. La Haye, G. McKee, T. W. Petrie, E. Doyle, G. Staebler, and M. R. Wade, "Gas puff fueled h-mode discharges with good energy confinement above the greenwald density limit on diii-d," *Physics of Plasmas*, vol. 8, no. 5, pp. 2017–2022, 2001. [Online]. Available: https://doi.org/10.1063/1.1345504

71. S. Mordijck, "Overview of density pedestal structure: role of fueling versus transport," *Nuclear Fusion*, vol. 60, no. 8, p. 082006, jul 2020. [Online]. Available: https://doi.org/10.1088/1741-4326/ab8d04

72. T. Eich, R. Goldston, A. Kallenbach, B. Sieglin, H. Sun, and and, "Correlation of the tokamak h-mode density limit with ballooning stability at the separatrix," *Nuclear Fusion*, vol. 58, no. 3, p. 034001, jan 2018. [Online]. Available: https://doi.org/10.1088/1741-4326/aaa340

73. A. Brown and R. Goldston, "Generalization of the heuristic drift sol model for finite collisionality and effect on flow shearing rate vs. interchange growth rate," *Nuclear Materials and Energy*, vol. 27, p. 101002, 2021. [Online]. Available: https://doi.org/10.1016/j.nme.2021.101002

74. L. Schmitz, K. Callahan, T. Rhodes, L. Zeng, Z. Yan, G. McKee, Y. Liu, T. Osborne, C. Chrystal, P. Gohil, B. Lyons, C. Petty, R. Wilcox, D. Shiraki, F. Laggner, S. Haskey, and B. Grierson, "Reduced L-H Transition Power Threshold in ITER-Similar-Shape DIII-D Hydrogen Plasmas*," in *APS Division of Plasma Physics Meeting Abstracts*, ser. APS Meeting Abstracts, vol. 2021, Jan. 2021, p. NO08.011. [Online]. Available: https://ui.adsabs.harvard.edu/abs/2021APS..DPPNO8011S